Neurocrit Care
https://doi.org/10.1007/s12028-018-0573-1

NEUROCRITICAL CARE SOCIETY

ORIGINAL ARTICLE

Detection of Brain Hypoxia Based on Noninvasive Optical Monitoring of Cerebral Blood Flow with Diffuse Correlation Spectroscopy

David R. Busch[1,2], Ramani Balu[3], Wesley B. Baker[1,4], Wensheng Guo[5], Lian He[1], Mamadou Diop[6], Daniel Milej[6], Venkaiah Kavuri[1], Olivia Amendolia[7], Keith St. Lawrence[6], Arjun G. Yodh[1] and W. Andrew Kofke[4*]

Abstract

Background: Diffuse correlation spectroscopy (DCS) noninvasively permits continuous, quantitative, bedside measurements of cerebral blood flow (CBF). To test whether optical monitoring (OM) can detect decrements in CBF producing cerebral hypoxia, we applied the OM technique continuously to probe brain-injured patients who also had invasive brain tissue oxygen (PbO_2) monitors.

Methods: Comatose patients with a Glasgow Coma Score (GCS) < 8) were enrolled in an IRB-approved protocol after obtaining informed consent from the legally authorized representative. Patients underwent 6–8 h of daily monitoring. Brain PbO_2 was measured with a Clark electrode. Absolute CBF was monitored with DCS, calibrated by perfusion measurements based on intravenous indocyanine green bolus administration. Variation of optical CBF and mean arterial pressure (MAP) from baseline was measured during periods of brain hypoxia (defined as a drop in PbO_2 below 19 mmHg for more than 6 min from baseline (PbO_2 > 21 mmHg). In a secondary analysis, we compared optical CBF and MAP during randomly selected 12-min periods of "normal" (> 21 mmHg) and "low" (< 19 mmHg) PbO_2. Receiver operator characteristic (ROC) and logistic regression analysis were employed to assess the utility of optical CBF, MAP, and the two-variable combination, for discrimination of brain hypoxia from normal brain oxygen tension.

Results: Seven patients were enrolled and monitored for a total of 17 days. Baseline-normalized MAP and CBF significantly decreased during brain hypoxia events ($p < 0.05$). Through use of randomly selected, temporally sparse windows of low and high PbO_2, we observed that both MAP and optical CBF discriminated between periods of brain hypoxia and normal brain oxygen tension (ROC AUC 0.761, 0.762, respectively). Further, combining these variables using logistic regression analysis markedly improved the ability to distinguish low- and high-PbO_2 epochs (AUC 0.876).

Conclusions: The data suggest optical techniques may be able to provide continuous individualized CBF measurement to indicate occurrence of brain hypoxia and guide brain-directed therapy.

Keywords: Brain ischemia, Hypoxia neuromonitoring, Cerebral ischemia, Hypoxia, Neuromonitoring, Clark electrode, Near-infrared spectroscopy, Diffuse correlation spectroscopy, Cerebral blood flow, Indocyanine green, Oxygen extraction fraction, Cerebral metabolic rate, Coma

*Correspondence: kofkea@uphs.upenn.edu
[4] Department of Anesthesiology and Critical Care, University of Pennsylvania, Philadelphia 19104, PA, USA
Full list of author information is available at the end of the article

Springer

Introduction

In present-day "state of the art" clinical care, critically ill patients are often admitted to the hospital with limited brain injury only to be discharged with significant neurologic disability caused by brain damage acquired during the hospital stay. This unsettling scenario occurs despite painstaking and expensive monitoring in the intensive care unit; it arises, in part, because we lack straightforward bedside methods to continuously monitor cerebral blood flow (CBF), especially its adequacy during progression of post-insult secondary brain damage. If detected early, decrements in CBF can potentially be treated to avert brain infarction. Unfortunately, the lack of widely applicable techniques for cerebral perfusion monitoring has resulted in clinicians making therapeutic decisions directed to non-neurologic endpoints such as blood pressure [1] and $PaCO_2$ [2] derived from population-based data, with expectations that such interventions will have a desired effect on an individual patient's brain perfusion.

Noninvasive optical monitoring (OM) of brain oxygenation holds potential to provide the necessary information to move from population-based to patient-based interventions. However, most examples of optical monitors currently available for clinical use (near-infrared spectroscopy [NIRS]) are incapable of absolute measurements of perfusion and metabolism. Previous work [3] comparing a commercial cerebral oximeter to invasive brain oxygen tension (PbO_2) [4] monitoring demonstrated a correlation between relative tissue oxygenation measured with the cerebral oximeter (rSO_2) and PbO_2; however, the confidence interval was wide, and the rSO_2 values were poor predictors of brain hypoxia measured with PbO_2. Previous reports by Rosenthal et al. [5] and Johnston et al. [6] have also demonstrated that PbO_2 is primarily sensitive to CBF linked to blood pressure [6]. Thus, a noninvasive tool to monitor CBF may be superior to devices measuring tissue oxygenation for predicting brain hypoxia measured by PbO_2.

Diffuse correlation spectroscopy (DCS) and diffuse optical spectroscopy (DOS) are promising noninvasive optical techniques [7], which can provide continuous bedside readouts of relative changes in CBF and tissue oxygenation [8, 9]. In this group of neurointensive care unit patients with invasive PbO_2 [4] monitoring, we first measured the transit of intravenously injected indocyanine green (ICG) boluses in brain tissue to calibrate relative changes in DCS signal to absolute CBF. We then tested the hypothesis that this novel noninvasive OM instrumentation can detect periods of brain hypoxia induced by insufficient levels of CBF. We focused on the ability of DCS to detect changes in brain tissue oxygen, given the aforementioned previous studies showing that cerebral blood flow is a major predictor of brain tissue oxygen tension.

Methods

Comatose patients (Glasgow Coma Score [GCS] ≤ 8) with traumatic brain injury, subarachnoid hemorrhage (SAH), intracerebral hemorrhage, or post-ischemic/anoxic encephalopathy who underwent invasive multimodality neuromonitoring as part of their standard care in the neuro-intensive care unit were eligible for enrollment in this observational study. Invasive neuromonitoring at our institution includes placement of a parenchymal intracranial pressure (ICP) monitor (Camino, Integra LifeSciences, Plainsboro, NJ, USA) and a brain tissue oxygen (P_bO_2) probe (Licox, Integra LifeSciences, Plainsboro, MA, USA) into frontal lobe white matter through a quad lumen bolt (Hemedex, Cambridge, MA, USA). In some patients, a cerebral microdialysis (CMD) probe (M Dialysis, North Chelmsford, MA, USA) and a thermodilution CBF monitor (Bowman Perfusion Monitor, Hemedex, Cambridge, MA, USA) were also placed; however, given the variability in usage of CMD and CBF monitors across enrolled patients, we focused on the capability of noninvasive OM to detect episodes of decreased CBF associated with brain hypoxia in this initial validation study. Clinical physiological data (including blood pressure, heart rate, end-tidal CO_2, oxygen saturation, and data from intracranial monitors) were continuously recorded onto a bedside monitor (CNS Monitor, Moberg Research, Ambler, PA, USA) for subsequent off-line analysis.

Optical CBF Monitoring

CBF measurements were made using DCS [7, 8]. The OM sensor was secured on the scalp over the frontal cortex area on the same hemisphere as the bolt (Fig. 1). DCS estimates blood flow by quantifying rapid speckle intensity fluctuations of multiply scattered light through tissue induced by red blood cell motion [10–13] (Fig. 2a). Specifically, DCS measures the normalized temporal intensity autocorrelation function, $g_2(\Delta t) = \langle I(t)I(t+\Delta t)\rangle / \langle I(t)\rangle^2$, at multiple delay times, Δt. Here, $I(t)$ is the detected light intensity at time t, and the angular brackets, $\langle\rangle$, represent time averages (in this study, an averaging time of 10 s was used). We employ a semi-infinite homogenous tissue model to derive a DCS blood flow index, F, from the decay of $g_2(\Delta t)$ (Fig. 2b). The DCS blood flow index, F, and its relative changes have been validated to be proportional to tissue blood flow against a plethora of gold-standard techniques [12, 14]. In our study, the relative changes in blood flow calculated by DCS were converted to "absolute" CBF values by calibration against a concurrent and colocated NIRS measurement of the transit of intravenously injected ICG through brain tissue. Each monitoring day, a single time point

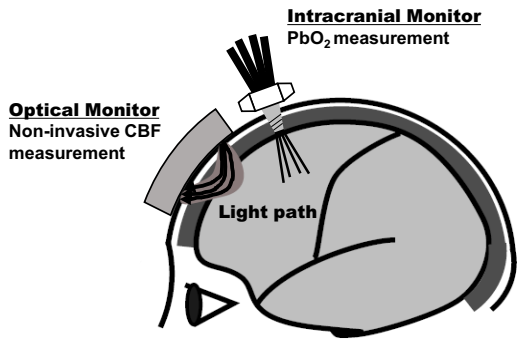

Fig. 1 Configuration of optical monitoring probe and intracranial monitors. The optode was placed on the forehead adjacent to the intracranial monitoring bolt

estimate of absolute CBF was derived by monitoring cerebral and arterial ICG concentrations following intravenous bolus administration (0.1 mg/kg, injected in < 3 s), as described previously by Diop et al. [15] and He et al. [16] and as illustrated in Fig. 3. This dynamic contrast-enhanced approach for measurement of CBF has been validated in preclinical studies [15] and in healthy humans [17].

The custom-built OM instrument consists of time-resolved DOS (TR-DOS) and DCS modules [18]. The TR-DOS light source is a commercial supercontinuum fiber laser (SuperK Extreme EXR-20, NKT Photonics Inc, Morganville, NJ, USA) that emits short white-light pulses (400–2400 nm, seed pulse width ~ 5 ps) at a repetition rate of 78 MHz. The fiber laser is coupled through an acousto-optic tunable filter (SuperK Cross, NKT Photonics Inc) for programmable selection of specific wavelengths to deliver to tissue via a SuperK Connect fiber delivery system (FD7, NKT Photonics Inc). Hybrid single-photon sensitive photomultiplier tubes (PMA hybrid 50, Picoquant Photonics Inc, Berlin, Germany) connected to a time-correlated single-photon counting module (HydraHarp 400, Picoquant Photonics Inc) were employed for TR-DOS photon time-of-flight measurements (1 ps resolution). Note the PMA hybrid detector was equipped with an electrically controlled shutter that was open only during TR-DOS acquisition.

The DCS light source is a continuous-wave, long-coherence length (≥ 8 m) 785-nm diode laser (IBEAM-SMART-785-S-WS with Smartdock fiber coupler, Toptica Photonics Inc, Victor, NY, USA) connected to a fiber-coupled electrically controlled shutter (OZ Optics, Ottawa, Ontario, Canada) for time-gated light delivery to tissue. DCS measurements of near-infrared light intensity autocorrelation functions (10 Hz sampling rate) were made with four arrays of four high-sensitivity

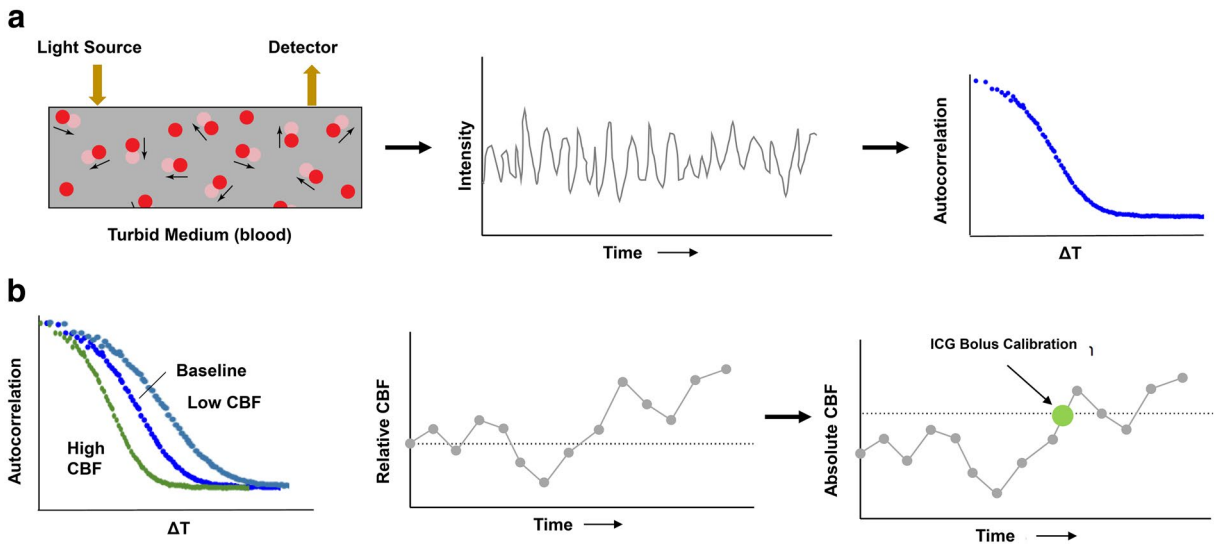

Fig. 2 Method of ICG-calibrated diffuse correlation spectroscopy (DCS) for absolute, real-time CBF measurements. **a** An infrared light source is used to probe turbid media with moving particles (i.e., red blood cells; red disks at time t, light red disks at time $t + \Delta t$). Specifically, light propagates diffusively through the tissue along random walk pathways and is scattered by moving red blood cells. The light scattered back from the tissue is measured at a detector placed adjacent to the source (source–detector separation is 2.5 cm). In our studies, the source/detector combination was incorporated into a single noninvasive optode patch. Light scattering by moving particles induces rapid (i.e., μs) temporal fluctuations in the detected speckle intensity, which are quantitatively characterized by the normalized intensity autocorrelation function. **b** Changes in the decay of the autocorrelation function over time are due to changes in CBF, which allows for a relative CBF index to be calculated over time. The rCBF index can be converted to absolute CBF by concurrent near-infrared spectroscopic measurement of the transit of ICG through brain tissue using the same optode [15]

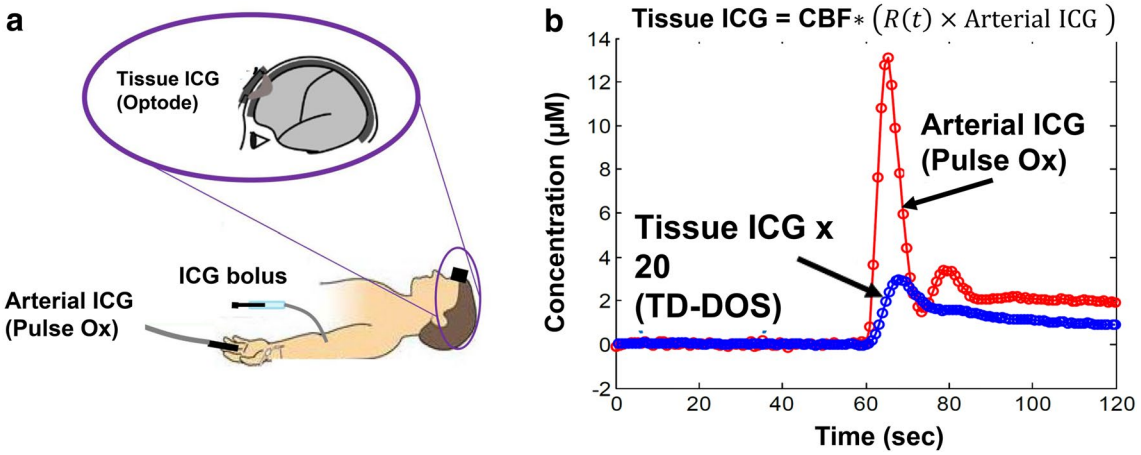

Fig. 3 Overview of method used for ICG-calibrated NIRS for absolute CBF measurement. **a** An intravenous bolus of ICG is given (0.1 mg/kg), and the temporal ICG concentration is measured in the arterial circulation via a custom pulse oximeter (or dye densitometer, with wavelengths of 804 and 938 nm that are optimal for ICG measurement) and in brain tissue via time-resolved DOS (using the optode with a source–detector separation of 3.2 cm, wavelength of 810 nm). The arterial and brain tissue ICG concentrations were sampled at 1 Hz. **b** Example of brain tissue ICG and arterial impulse response function from a patient is shown. Tissue ICG concentration is equivalent to the convolution of the arterial impulse response (i.e., the arterial ICG concentration) and CBF × $R(t)$, where $R(t)$ is the fraction of ICG that remains in tissue at time t. Absolute CBF is calculated by deconvolving the tissue ICG concentration with the arterial ICG concentration to obtain CBF × $R(t)$, and then taking the $t=0$ intercept (since $R(0)=1$ by definition)

single-photon counting avalanche photodiodes (Excelitas SPCM-AQ4C, Pacer LLC, Palm Beach Gardens, FL, USA) connected to a multiple-τ 16-channel hardware correlator (Correlator.com, Bridgewater, NJ, USA) operating in burst mode [19]. For more details about DCS and TR-DOS instrumentation, we refer readers to recent reviews [8, 20, 21]. Optical fibers couple the DCS and TR-DOS light sources and detectors to the OM sensor secured to the head. In this report, a DCS source–detector separation of 2.5 cm and a TR-DOS source–detector separation of 3.2 cm were used.

Statistical Analyses

From enrollment to removal of the brain bolt, patients underwent 6–8 h of daily OM. We assessed the ability of noninvasive optical CBF monitoring to detect CBF decrements associated with brain hypoxia using two analytic approaches. In the first approach, we identified discrete episodes of brain hypoxia defined as decrement to $PbO_2 < 19$ mmHg [4, 22, 23] for > 6 min from a baseline $PbO_2 > 21$ mmHg for > 6 min (Fig. 4), and we compared these brain hypoxia episodes with OM changes in CBF and with changes in mean arterial pressure (MAP) (one-minute time windows). A Wilcoxon signed-rank test was used to compare distributions.

The second analytic approach evaluated randomly selected periods of "low" (≤ 19 mmHg) and "normal" (≥ 21 mmHg) PbO_2 from all of the monitoring days. For each of the monitoring days, we randomly selected up to four 12-min periods of "low" PbO_2 at least 120-min apart and up to four 12-min periods of "normal" PbO_2, again separated by at least 120 min. Given this temporal separation, each period was considered independent of any other period: as data collected in one window are unlikely to be correlated with those in another. Each period was thus considered independent of any other period.

Receiver operator characteristic curves were plotted to assist in screening potential noninvasive variables which might predict low PbO_2.

Results

Seven patients with GCS < 8 were enrolled with the following diagnoses: traumatic brain injury ($n=3$), intracerebral hemorrhage ($n=2$), and post-ischemic encephalopathy ($n=2$). The entire cohort underwent concurrent noninvasive OM for a total of 17 days. Each measurement day was considered independent.

Overall, both MAP and DCS-CBF showed a significant correlation with PbO_2 (Fig. 5) but with noticeable inter- and intra-subject variation. A total of 17 brain hypoxia events (as defined by the PbO_2 changes described above) were identified in three of the seven patients studied (Table 1). During the brain hypoxia events, we observed (Fig. 6) significant changes in MAP ($p=0.0004$) as well as CBF ($p=0.01$, normalized to pre-event baseline). Further, since we performed simultaneous TD-DOS measurements, we were able to analyze whether brain hypoxia was associated with drops in regional oxygen saturation (rSO_2).

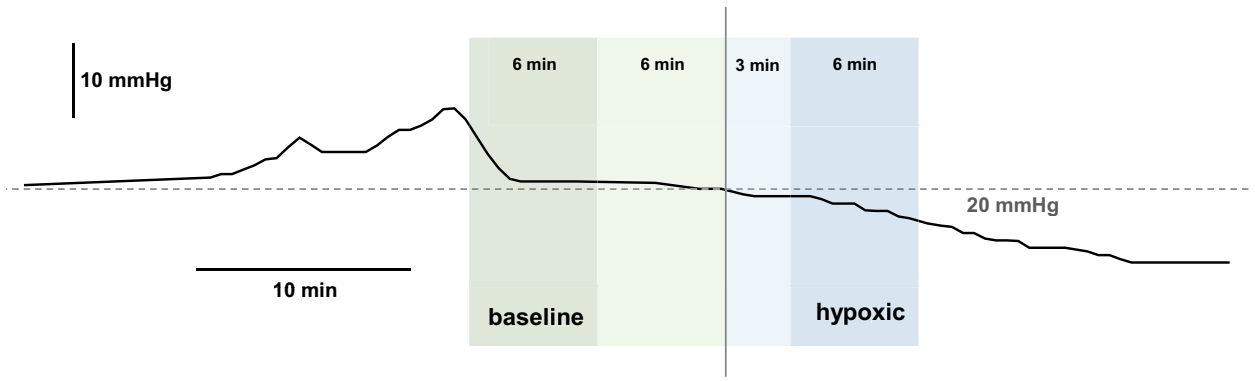

Fig. 4 Method for identifying hypoxic events. The plot shows ~1 h of continuous PbO_2 data from subject OM-14. An episode of brain hypoxia was defined as the average PbO_2 in a 6-min period of sustained $PbO_2 < 20$ mmHg that followed a 3-min period where PbO_2 transitioned from > 20 mmHg to < 19 mmHg. The pre-hypoxia baseline was defined as the average PbO_2 in a 6-min period of time that occurred 6 min prior to the transition to brain hypoxia

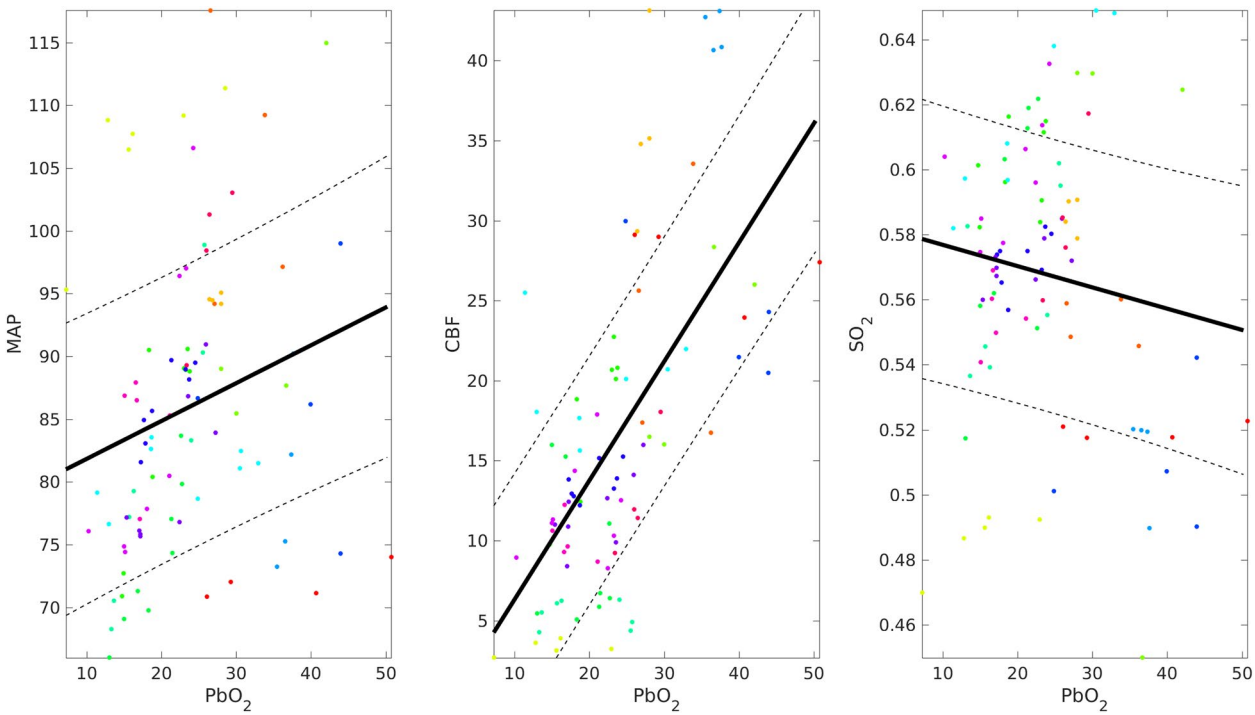

Fig. 5 Scatter plot of MAP (mmHg), CBF (ml/100 g/min), and SO_2 (fraction) versus PbO_2 (mmHg) for randomly selected windows 12-min long (as discussed in the text). Fit lines and 95% confidence intervals are shown in black. CBF is substantially more sensitive to changes in PbO_2 than either of the other variables

Interestingly, rSO_2 values were not significantly associated with episodes of brain hypoxia on PbO_2 (AUC 0.46), with only a modest inverse correlation observed (Fig. 5).

Our second analysis utilized randomly selected, temporally sparse windows of low and high PbO_2. Low PbO_2 episodes were identified in 3/7 patients ($n = 36$ episodes), while normal PbO_2 episodes were identified in all patients ($n = 58$ episodes) (Table 1). We found that both MAP and changes in CBF discriminated between periods of brain hypoxia and normal brain oxygen tension (AUC 0.761, 0.762, respectively) (Fig. 7). We next employed logistic regression to derive a weighted linear combination of these parameters that optimized separation of the high and low windows (Log odds of

Table 1 Summary of patient demographics, diagnoses, and contributions of each patient to the various types of PbO_2 episodes

ID	Age	Gender	Diagnosis	Days monitored	Brain hypoxia episodes	Low PbO_2 episodes	Normal PbO_2 episodes
3	29	Male	TBI	3	0	0	12
4	63	Female	ICH	2	2	4	2
5	38	Female	PIAE	1	0	0	4
6	33	Male	PIAE	4	10	16	15
12	49	Female	TBI	2	0	0	8
14	62	Male	ICH	4	5	16	13
15	27	Male	TBI	1	0	0	4

ICH intracerebral hemorrhage, *PIAE* post-ischemic/anoxic enceplopathy, *TBI* traumatic brain injury

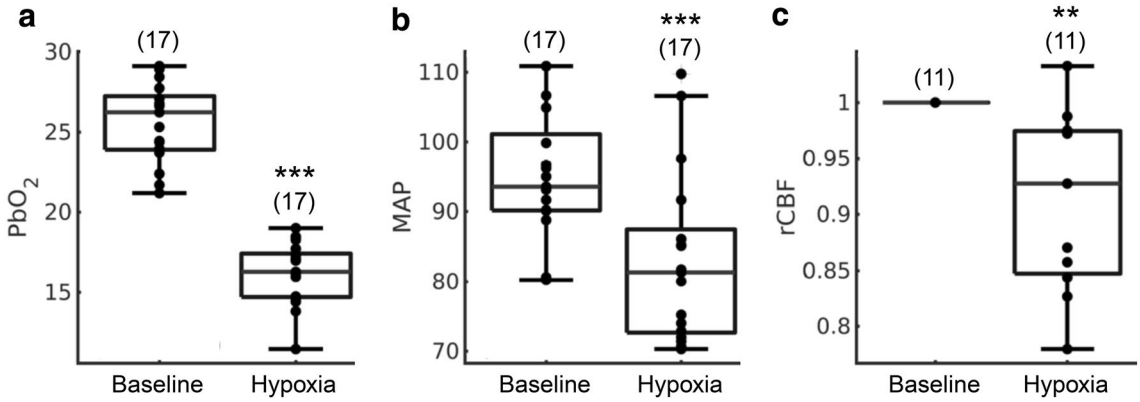

Fig. 6 **a** Brain tissue oxygen measurements during hypoxic events, **b** mean arterial pressure (MAP), and **c** cerebral blood flow relative to baseline (rF = CBF/$CBF_{Baseline}$)] during hypoxic events. Median baseline CBF was 13.9 ml/100gm/min (IQR 8.6:16.5). MAP ($p = 0.00035$) and rF ($p = 0.01$) are significantly lower during hypoxic events. ***$p < 0.001$; **$p < 0.01$

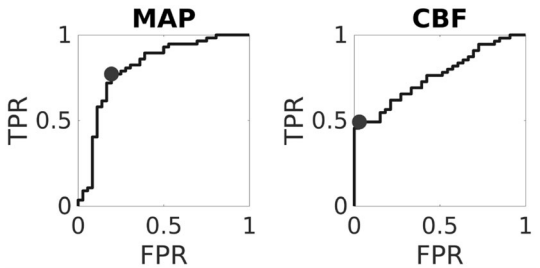

Fig. 7 Receiver operating characteristic (ROC) curves for MAP and optically measured CBF to separate randomly and sparsely chosen windows of low and high PbO_2. MAP and absolute CBF were associated with low PbO_2 (ROC AUC 0.761, 0.762, respectively). Combining these variables using logistic regression analysis markedly improved the ability to distinguish low and high PbO_2 epochs (AUC 0.876). *TPR* true positive rate, *FPR* false positive rate

low $PbO_2 = -18.0202 + 0.1805 * MAP + 0.2191 * CBF$, all coefficients significant at $p < 0.05$). This combined MAP and CBF data type improved our ability to discriminate between high and low PbO_2 episodes (AUC 0.876) compared to either variable alone.

Conclusion

Invasive PbO_2 monitoring is frequently used to guide care in patients with acute brain injury, and when combined with ICP monitoring, it may play an important role in providing personalized care which may affect outcome. Stiefel et al. [4] showed an association between low PbO_2 episodes and outcome after traumatic brain injury, and this observation has been supported by other reports [23, 24]. Unfortunately, due to multiple factors, invasive neuromonitoring is only feasible for a small subset of patients with severe acute brain injury. Our data support the notion that noninvasive OM of CBF may provide a useful surrogate indicator of brain hypoxia, thus enabling the identification of physiological states that are associated with secondary brain injury in patients for which it is not possible to place invasive monitors. While encouraging however, given the small sample size and lack of an independent test set, we urge the reader to be cautious about the generalizability of these findings. More work with larger samples sizes is needed.

To summarize, we found that reductions in both optical CBF and blood pressure predicted episodes of brain

hypoxia. Changes in PbO_2 reflect the combined effect of changes in cerebral blood flow, blood pressure, and levels of dissolved free plasma oxygen [5, 6]. For example, hyperventilation produces decrements in PbO_2 by reducing CBF, while hyperoxia [5], transfusion [25], and increasing blood pressure [5, 6] can all cause an increase in PbO_2 through multiple complementary mechanisms. Overall, these observations are consistent with our findings and support the view that reductions in PbO_2 reflect multiple potentially adverse conditions, including reductions in cerebral perfusion and factors (such as reduced blood pressure) that contribute to low CBF states. Interestingly, we found that regional oxygen saturation (measured noninvasively by concurrent TD-DOS) did not predict brain hypoxia (i.e., low PbO_2). Although counterintuitive, this finding partially agrees with a previous study comparing invasive $PbtO_2$ to measurements of rSO_2 with a commercial NIRS instrument [3]. While rSO_2 and PbO_2 were correlated in that study, the rSO_2 changes were not sufficiently sensitive to reliably detect episodes of brain hypoxia. The decreased sensitivity of NIRS compared to DCS may be due to the fact that NIRS and invasive PbO_2 are measuring oxygenation in different brain compartments (blood and interstitial fluid, respectively), or that NIRS rSO_2 requires an assumption on the arteriovenous admixture, where the signal is dominated by capillaries and venules [9]. Assuming no change in tissue blood volume, the total blood flow in each vascular compartment is equal and therefore the precise compartmental contributions to the DCS signal will not influence the measurement. When blood volume is changing, high-temporal resolution DCS has demonstrated that pulsatile flow dominates the signal, suggesting that the arteriole contribution dominates DCS blood flow measurements [26]. Note that NIRS and DCS can provide complementary information on hypoxic brain states, with NIRS more faithfully reporting episodes due to systemic hypoxia or increased cortical cerebral metabolic demand and DCS reporting episodes caused by decreased cerebral perfusion. Further work is required to clarify these issues.

The observation that both MAP and noninvasive CBF predict brain hypoxia episodes suggests that our patients had significant impairments of cerebral autoregulation. Further work is needed to ascertain whether similar results will be seen in patients with less severe forms of brain injury, for example, wherein autoregulation is relatively preserved. Our results also point to the possible use of continuous DCS as a means to extract a real-time, direct, flow-based index of pressure autoregulation, i.e., similar to autoregulation indices that are indirect and employ ICP [27], PbO_2 [28], and NIRS [29]. In a recently published study in healthy volunteers, we demonstrated the potential utility of DCS to monitor cerebral autoregulation [26], and we plan to investigate the feasibility of DCS to continuously measure autoregulation in brain-injured patients.

The noninvasive OM we used is a promising technology for neurocritical care. DCS is an alternative method for assessing CBF that has light penetration properties similar to near-infrared spectroscopy (NIRS) cerebral oximeters (e.g., Casmed FORE-SIGHT Elite, Covidien INVOS 5100C, Masimo O3, Hamamatsu NIRO, etc.). DCS extracts a blood flow index from measurement of temporal fluctuations in the reflected light intensity primarily caused by moving red blood cells (Fig. 1). However, while the light utilized for NIRS, time-domain optical bolus tracking, and DCS is similar in wavelength and tissue penetration, there are differences in in-depth sensitivity. Continuous illumination NIRS is most sensitive to superficial tissues (e.g., skin, scalp), while the additional information provided by both time-domain and dye bolus measurements permits greater selective sensitivity to deeper tissues. DCS utilizes a fundamentally different contrast—moving red blood cells instead of hemoglobin absorption—and its depth sensitivity is correspondingly weighted by the blood flow at each depth. In the brain, blood flow is many times higher than that of the skull/scalp, increasing DCS sensitivity to cerebral blood flow [30].

Our data suggest that DCS can likely detect an anaerobic condition, and, notably, it does not rely on assumptions regarding microcirculatory arteriovenous admixture [9] as is the case with traditional NIRS cerebral oximeters. NIRS oximeters reflect an uncertain mixture of artery, capillary, and venous blood, and the precise arterial and venous contributions can vary within and across patients [31]. These assumptions limit establishment of quantitative NIRS oximetry saturation thresholds for ischemia. Relative and absolute quantitative CBF measurements with DCS, however, are not subject to this limitation, because the technique is based on assessment of erythrocyte movement rather than hemoglobin-based light absorption, and total blood flow in each microvasculature compartment must be the same, in the absence of change in tissue blood volume. Future work will be required to confirm our observations and establish ischemic CBF thresholds, for example, by expanding study populations and utilizing more sophisticated statistical models to account for potential intra-subject correlations.

The initial generation of DCS technology for assessing relative CBF has been validated in multiple contexts. Initial proof of concept evaluation entailed extensive studies in tissue phantoms [10] wherein the medium's viscosity and therefore thermal motion of scatterers could be controlled. In subsequent reports, investigators compared

DCS measurements of flow variation to other standards including Doppler ultrasound [32], laser Doppler [33], and perfusion magnetic resonance (MR) imaging [34]. In rodents, DCS detected hyperemia due to hypercapnia [35, 36] and ischemia due to cardiac arrest [36] with appropriate changes in oxygen extraction fraction (OEF) and $CMRO_2$ [36]. DCS-detected changes in CBF have been reported in still other animal studies [12, 37], including comparison with contrast-enhanced time-domain CBF measurements [15], and also with stable xenon-enhanced computed tomography (CT) in SAH patients [14] and MR-based validation in children [13]. Overall, these and numerous other uncited validation studies demonstrated that DCS measurements of blood flow variations in humans are in reasonable agreement with theoretical expectation and with other measurement techniques. Our results presented here (e.g., Fig. 6) corroborate these findings and further support the study of DCS-detected changes in CBF to inform clinical care.

Incorporation of a time-domain near-infrared analysis with ICG intravenous injection has enabled quantitative calibration of absolute CBF for DCS. This calibration approach has been validated in a preclinical study in neonatal piglets versus perfusion CT [15] and in healthy humans with MR arterial spin labeling CBF assessment [17], though more work remains. Our data using a semi-infinite medium calculation method add to this literature by assessing absolute CBF in comparison with invasive PbO_2. Future work will include the use of layered models to remove possible signal contamination from the scalp; [38] we, and others, are exploring adaptations of these techniques suitable for critically ill patients with invasive monitors. Moreover, the stability of the DCS calibration for continuous absolute CBF monitoring with DCS has been tested via a second absolute CBF measurement with ICG injection roughly 4 h after the calibration measurement [16]. This test confirms stability of calibration over at least 4 h of monitoring. This development of quantitative CBF monitoring, combined with assessment of SaO_2 and tissue O_2 saturation, additionally provides for the possibility of a monitor of quantitative $CMRO_2$ and OEF. Quantitative CBF monitoring by DCS with ICG calibration is much less well studied than relative measurements of CBF with DCS; as further results emerge, it may prove to offer additional benefit to clinical decision making.

Our data suggest that optical techniques can provide continuous individualized regional CBF measurement to guide brain-directed therapy to avoid anaerobic conditions. Given our small sample size, the need for expanded clinical studies of noninvasive tools is apparent, both to improve the care of those who currently undergo invasive monitoring and also care for other patients, without invasive monitoring, but at risk of neurologic deterioration.

Author details
[1] Department of Physics and Astronomy, University of Pennsylvania, Philadelphia, PA, USA. [2] Departments of Anesthesiology and Pain Management & Neurology and Neurotherapeutics, University of Texas, Southwestern Medical Center, Dallas, TX, USA. [3] Department of Neurology, University of Pennsylvania, Philadelphia, PA, USA. [4] Department of Anesthesiology and Critical Care, University of Pennsylvania, Philadelphia 19104, PA, USA. [5] Department of Biostatistics and Epidemiology, University of Pennsylvania, Philadelphia, PA, USA. [6] Department of Medical Biophysics, Lawson Health Research Institute, University of Western Ontario, London, Canada. [7] Neurosurgery Clinical Research Division, Hospital of the University of Pennsylvania, Philadelphia, PA, USA.

Authors' Contributions
DRB and WG are involved in data analysis, conceptualization of protocol, and manuscript composition contribution; RB, data analysis, patient recruitment, conceptualization of protocol, and manuscript composition contribution); WBB, data analysis, collection and organization of patient data, ICG CBF analysis, conceptualization of protocol, and manuscript composition contribution; LH, building and maintaining of instrumentation, collection and maintenance of patient data, ICG CBF analysis, and manuscript composition contribution; MD, DM, and KSL, ICG CBF analysis, manuscript composition contribution; VK, instrument construction and bioengineering; OA, data collection and management, patient enrollment, manuscript composition contribution; AGY, biomedical optics, physics and analysis oversight, conceptualization of protocol, manuscript composition contributions; WAK, conceptualization of protocol, clinical oversight, patient recruitment, and manuscript composition contribution.

Source of support
We acknowledge support from the National Institute of Health (R01-NS082309-01A1, R01-NS060653, P41-EB015893).

Compliance with Ethical Standards

Conflict of interest
Several of the investigators received salary support from the National Institutes of Health, Canadian Institutes of Health Research, and the National Science Foundation; Wesley B. Baker has submitted two Patents to the US Patent office on behalf of the Trustees of the University of Pennsylvania: provisional patent number 17-8261/103241.000816, and provisional patent number 14-6924/103241.005919; Ramani Balu has participated in a patent submitted to the US Patent office on behalf of the Trustees of the University of Pennsylvania, US20160361017A1; Mamadou Diop, Olivia Amendolia, Wensheng Guo, Keith St. Lawrence, have no additional conflicts of interest to disclose; Venkaiah Kavuri works for Masimo, a biooptics corporation and has a patent US20170049417A1 pending on behalf of the University of Texas System; W. Andrew Kofke is on the editorial board of the Journal of Neurosurgical Anesthesiology and is on the editorial board of Neurocritical Care, and he has participated in a patent submitted to the US Patent office on behalf of the Trustees of the University of Pennsylvania: provisional patent number 17-8261/103241.000816; Arjun G. Yodh has his name is on eight patents submitted on behalf of the Trustees of the University of Pennsylvania, US6304771B1, US5917190A, US6076010A, US20080292164A1, US20060063995A1, US6487428B1, US6831741B1, and provisional patent number 17-8261/103241.000816. David R. Busch has a International Patent Applications PCT/US2015/017277 and PCT/US2015/017286.

Ethical Approval
The Institutional Review Board of the University of Pennsylvania approved all aspects of the study. All procedures performed were in accordance with the ethical standards of the 1964 Helsinki declaration and its later amendments or comparable ethical standards. Informed consent was obtained from all individual participants' legally authorized representatives.

Published online: 20 July 2018

References

1. Anderson CS, Heeley E, Huang Y, et al. Rapid blood-pressure lowering in patients with acute intracerebral hemorrhage. N Engl J Med. 2013;368:2355–65.
2. Muizelaar J, Marmarou A, Ward J, et al. Adverse effects of prolonged hyperventilation in patients with severe head injury: a randomized clinical trial. J Neurosurg. 1991;75:731–9.
3. Leal-Noval SR, Cayuela A, Arellano-Orden V, et al. Invasive and noninvasive assessment of cerebral oxygenation in patients with severe traumatic brain injury. Intensive Care Med. 2010;36:1309–17.
4. Stiefel M, Spiotta A, Gracias V, et al. Reduced mortality rate in patients with severe traumatic brain injury treated with brain tissue oxygen monitoring. J Neurosurg. 2005;103:805–11.
5. Rosenthal G, Hemphill JC III, Sorani M, et al. Brain tissue oxygen tension is more indicative of oxygen diffusion than oxygen delivery and metabolism in patients with traumatic brain injury. Crit Care Med. 2008;36:1917–24.
6. Johnston AJ, Steiner LA, Coles JP, et al. Effect of cerebral perfusion pressure augmentation on regional oxygenation and metabolism after head injury. Crit Care Med. 2005;33:189–95.
7. Yodh AG, Greenberg JG, Yu G, et al. Inventors; Optical Measurement of Tissue Blood Flow, Hemodynamics and Oxygenation, US Patent 8,082,015; 2011.
8. Durduran T, Yodh AG. Diffuse correlation spectroscopy for non-invasive, micro-vascular cerebral blood flow measurement. Neuroimage. 2014;85:51–63.
9. St Lawrence K, Verdecchia K, Elliott J, Diop M. Measuring cerebral hemodynamics and energy metabolism by near-infrared spectroscopy., NeuromethodsNew York: Humana Press Inc.; 2014. p. 265–92.
10. Boas DA, Campbell LE, Yodh AG. Scattering and imaging with diffusing temporal field correlations. Phys Rev Lett. 1995;75:1855–8.
11. Boas DA, Yodh AG. Spatially varying dynamical properties of turbid media probed with diffusing temporal light correlation. J Opt Soc Am A. 1997;14:192–215.
12. Zhou C, Eucker SA, Durduran T, et al. Diffuse optical monitoring of hemodynamic changes in piglet brain with closed head injury. J Biomed Opt. 2009;14:034015.
13. Buckley EM, Hance D, Pawlowski T, et al. Validation of diffuse correlation spectroscopic measurement of cerebral blood flow using phase-encoded velocity mapping magnetic resonance imaging. J Biomed Opt. 2012;17:037007.
14. Kim MN, Durduran T, Frangos S, et al. Noninvasive measurement of cerebral blood flow and blood oxygenation using near-infrared and diffuse correlation spectroscopies in critically brain-injured adults. Neurocrit Care. 2010;12:173–80.
15. Diop M, Verdecchia K, Lee TY, St Lawrence K. Calibration of diffuse correlation spectroscopy with a time-resolved near-infrared technique to yield absolute cerebral blood flow measurements. Biomed Opt Express. 2011;2:2068–82.
16. He L, Baker W, Kavuri V, et al. Noninvasive optical monitoring of absolute cerebral blood flow in adult human subjects (abstract). J Neurosurg Anesthesiol. 2017;29:494.
17. Milej D, He L, Abdalmalak A, et al. Quantification of cerebral blood flow in adults by dynamic contrast-enhanced NIRS: validation against MRI. In Biophotonics congress: biomedical optics congress 2018 (Microscopy/Translational/Brain/OTS), OSA technical digest (Optical Society of America, 2018), paper BF2C.2. 2018. https://doi.org/10.1364/BRAIN.2018.BF2C.2.
18. Kavuri VC, Baker W, Parthasarathy AB, Balu R, Yodh AG, Kofke A. A combined diffuse correlation and time-resolved spectroscopy instrument for continuous monitoring of absolute cerebral blood flow. Biomedical Optics 2016; 2016 2016/04/25; Fort Lauderdale, Florida: Optical Society of America. p. JW3A.8.
19. Dietsche G, Ninck M, Ortolf C, Li J, Jaillon F, Gisler T. Fiber-based multispeckle detection for time-resolved diffusing-wave spectroscopy: characterization and application to blood flow detection in deep tissue. Appl Opt. 2007;46:8506.
20. Torricelli A, Contini D, Pifferi A, et al. Time domain functional NIRS imaging for human brain mapping. Neuroimage. 2014;85:28–50.
21. Pifferi A, Contini D, Mora AD, Farina A, Spinelli L, Torricelli A. New frontiers in time-domain diffuse optics, a review. J Biomed Opt. 2016;21:091310.
22. Le Roux P, Menon DK, Citerio G, et al. Consensus summary statement of the international multidisciplinary consensus conference on multimodality monitoring in neurocritical care: a statement for healthcare professionals from the Neurocritical Care Society and the European Society of Intensive Care Medicine. Intensive Care Med. 2014;40:1189–209.
23. Oddo M, Levine JM, MacKenzie L, et al. Brain hypoxia is associated with short-term outcome after severe traumatic brain injury independently of intracranial hypertension and low cerebral perfusion pressure. Neurosurgery. 2011;69:1037–45.
24. Spiotta AM, Stiefel MF, Gracias VH, et al. Brain tissue oxygen-directed management and outcome in patients with severe traumatic brain injury. J Neurosurg. 2010;113:571–80.
25. Smith M, Maggee S, Stiefel M, Bloom S, Gracias V, Le Roux P. Packed red blood cell transfusion increases local cerebral oxygenation. Crit Care Clin. 2005;33:1104–8.
26. Parthasarathy AB, Gannon KP, Baker WB, et al. Dynamic autoregulation of cerebral blood flow measured non-invasively with fast diffuse correlation spectroscopy. J Cereb Blood Flow Metab. 2018;38:230–40.
27. Czosnyka M, Smielewski P, Kirkpatrick P, Laing RJ, Menon D, Pickard JD. Continuous assessment of the cerebral vasomotor reactivity in head injury. Neurosurgery. 1997;41:11–7.
28. Menzel M, Soukup J, Henze D, et al. Brain tissue oxygen monitoring for assessment of autoregulation: preliminary results suggest a new hypothesis. J Neurosurg Anesthesiol. 2003;15:33–41.
29. Zweifel C, Castellani G, Czosnyka M, et al. Continuous assessment of cerebral autoregulation with near-infrared spectroscopy in adults after subarachnoid hemorrhage. Stroke. 2010;41:1963–8.
30. Selb JJ, Boas DA, Chan S-T, Evans KC, Buckley EM, Carp SA. Sensitivity of near-infrared spectroscopy and diffuse correlation spectroscopy to brain hemodynamics: simulations and experimental findings during hypercapnia. Neurophotonics. 2014;1:015005.
31. Watzman HM, Kurth CD, Montenegro LM, Rome J, Steven JM, Nicolson SC. Arterial and venous contributions to near-infrared cerebral oximetry. Anesthesiology. 2000;93:947–53.
32. Yu G, Durduran T, Zhou C, et al. Noninvasive monitoring of murine tumor blood flow during and after photodynamic therapy provides early assessment of therapeutic efficacy. Clin Cancer Res. 2005;11:3543–52.
33. Durduran T. Non-invasive measurements of tissue hemodynamics with hybrid diffuse optical methods. Thesis. Philadelphia: University of Pennsylvania; 2004.
34. Durduran T, Yu G, Burnett MG, et al. Diffuse optical measurement of blood flow, blood oxygenation, and metabolism in a human brain during sensorimotor cortex activation. Opt Lett. 2004;29:1766–8.
35. Cheung C, Culver JP, Takahashi K, Greenberg JH, Yodh AG. In vivo cerebrovascular measurement combining diffuse near-infrared absorption and correlation spectroscopies. Phys Med Biol. 2001;46:2053–65.
36. Culver JP, Durduran T, Cheung C, Furuya D, Greenberg JH, Yodh AG. Diffuse optical measurement of hemoglobin and cerebral blood flow in rat brain during hypercapnia, hypoxia and cardiac arrest. Adv Exp Med Biol. 2003;510:293–7.
37. Carp SA, Dai GP, Boas DA, Franceschini MA, Kim YR. Validation of diffuse correlation spectroscopy measurements of rodent cerebral blood flow with simultaneous arterial spin labeling MRI; towards MRI-optical continuous cerebral metabolic monitoring. Biomed Opt Express. 2010;1:553–65.
38. Baker WB, Parthasarathy AB, Ko TS, et al. Pressure modulation algorithm to separate cerebral hemodynamic signals from extracerebral artifacts. Neurophotonics. 2015;2:035004.